Imaging of pulmonary emphysema: A pictorial review

Masashi Takahashi[1]
Junya Fukuoka[2]
Norihisa Nitta[1]
Ryutaro Takazakura[1]
Yukihiro Nagatani[1]
Yoko Murakami[1]
Hideji Otani[1]
Kiyoshi Murata[1]

[1]Department of Radiology, Shiga University of Medical Science, Shiga, Japan; [2]Laboratory of Pathology, Toyama University Hospital, Toyama, Japan

Abstract: The term 'emphysema' is generally used in a morphological sense, and therefore imaging modalities have an important role in diagnosing this disease. In particular, high resolution computed tomography (HRCT) is a reliable tool for demonstrating the pathology of emphysema, even in subtle changes within secondary pulmonary lobules. Generally, pulmonary emphysema is classified into three types related to the lobular anatomy: centrilobular emphysema, panlobular emphysema, and paraseptal emphysema. In this pictorial review, we discuss the radiological – pathological correlation in each type of pulmonary emphysema. HRCT of early centrilobular emphysema shows an evenly distributed centrilobular tiny areas of low attenuation with ill-defined borders. With enlargement of the dilated airspace, the surrounding lung parenchyma is compressed, which enables observation of a clear border between the emphysematous area and the normal lung. Because the disease progresses from the centrilobular portion, normal lung parenchyma in the perilobular portion tends to be preserved, even in a case of far-advanced pulmonary emphysema. In panlobular emphysema, HRCT shows either panlobular low attenuation or ill-defined diffuse low attenuation of the lung. Paraseptal emphysema is characterized by subpleural well-defined cystic spaces. Recent topics related to imaging of pulmonary emphysema will also be discussed, including morphometry of the airway in cases of chronic obstructive pulmonary disease, combined pulmonary fibrosis and pulmonary emphysema, and bronchogenic carcinoma associated with bullous lung disease.

Keywords: pulmonary emphysema, HRCT, radiologic-pathologic correlation, pulmonary fibrosis, bronchus, lung cancer

Introduction

Chronic obstructive pulmonary disease (COPD) is a disease characterized by airflow limitation that is not fully reversible (Pauwels et al 2001). The pathogenesis of COPD is thought to be chronic inflammation throughout the airways, parenchyma, and pulmonary vasculature (Pauwels et al 2001). Pathologic changes characteristic of COPD occur in all these respiratory structures. Among these changes, destruction of the lung parenchyma is commonly referred to as pulmonary emphysema, defined as "an abnormal permanent enlargement of the air space distal to the terminal bronchioles, accompanied by destruction of the alveolar walls, and without obvious fibrosis" (ATS 1962; Snider et al 1985). The etiology of pulmonary emphysema has not been fully established (Tuder et al 2006), but the prevailing concept is that lung inflammation caused by cigarette smoke, environmental pollutants, or bacterial products leads to an imbalance of proteases and antiproteases (Tuder et al 2006). Although the traditional inflammatory cell implicated in emphysema is the neutrophil which releases neutorophil elastase, recent research has been focused on the macrophage and macrophage-derived protease (Wright and Churg 2007). The link between the inflammation and inflammation-related genes was also highlighted (Grumelli et al 2004). Apoptosis and oxidative stress also act as amplification mechanisms (Tuder et al 2006).

The term emphysema is generally used in a morphological sense in the field of pathology and radiology and should not be directly related with physiological impairment. Imaging modalities have an important role in diagnosis of pulmonary

Correspondence: Masashi Takahashi
Department of Radiology, Shiga University of Medical Science, Seta-Tsukinowa, Otsu, Shiga 520-2192, Japan
Tel +81 77 548 2288
Fax +81 77 544 0986
Email masashi@belle.shiga-med.ac.jp

emphysema, and high resolution computed tomography (HRCT) is an especially reliable tool for demonstrating the pathology of emphysema, even for subtle changes in secondary pulmonary lobules. In this pictorial review, we show the radiological – pathological correlation in pulmonary emphysema. Recent topics related to imaging of pulmonary emphysema will also be discussed, including morphometry of the airway in cases of COPD, combined pulmonary fibrosis and pulmonary emphysema, and bronchogenic carcinoma associated with bullous lung disease (BLD).

Anatomy of the secondary pulmonary lobule

An understanding of the normal anatomy of the peripheral lung is required when interpreting CT images of pulmonary emphysema. From the trachea, airways with a diameter of 1 mm reach the level of the lobular bronchus after 9 to 14 dichotomous branches. Lobular bronchus has 3 to 5 smaller airways, which are called terminal bronchioles (Figure 1). These bronchioles arise at intervals of 1 to 2 mm while prelobular bronchi arise at intervals of 0.5 to 1.0 cm (Reid 1958). A unit consisting of 3 to 5 terminal bronchioles supplied by a small bronchus with a diameter of 1 mm is called a secondary pulmonary lobule (Reid's lobule) (Reid 1958). Therefore, an intralobular region can be recognized if the branching distance

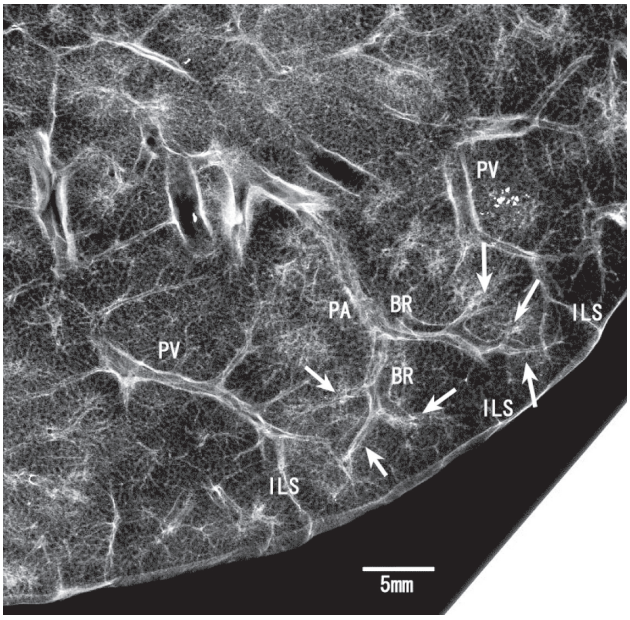

Figure 1 Secondary pulmonary lobule: Reid's definition. Contact radiograph of the inflated fixed lung specimen showing the branching terminal bronchioles (arrows). These terminal bronchioles arise at intervals of 1 to 2 mm. The bar represents 5 mm.
Abbreviations: BR, bronchus; PA, pulmonary artery; PV, pulmonary vein; ILS, interlobular septum.

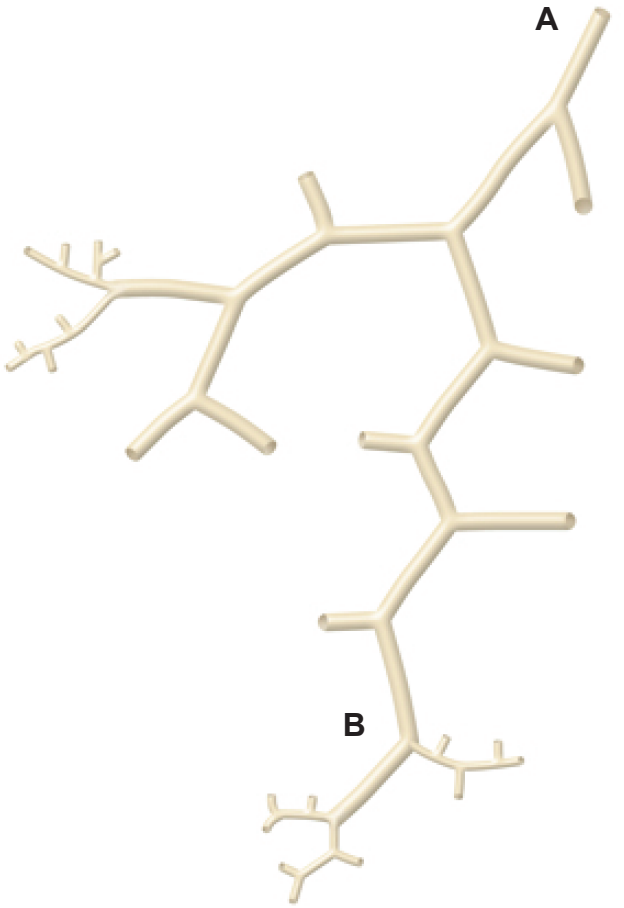

Figure 2 The cm and mm patterns. Diagram (modified from Reid) showing the branching pattern of the end of a bronchial pathway. Initially the branches arise at intervals of approximately 0.5 to 1.0 cm (**A** to **B**) and then arise at intervals of approximately 2 mm (beyond **B**). Copyright © 1958. Adapted and reproduced with permission from the BMJ Publishing Group, from Reid L. 1958. The secondary lobule in the adult human lung with special reference to its appearance in bronchograms. *Thorax*, 13:110–15.

Figure 3 Secondary pulmonary lobule: Miller's definition. Specimen photograph demonstrating a rich network of interlobular septa. Noted that the area surrounded by the septa is variable.
Abbreviation: PV, pulmonary vein.

is constant at 1 to 2 mm. Prelobular branching is referred to as a "cm pattern" and an intralobular pattern is called an "mm pattern" (Reid 1958) (Figure 2), and the area supplied by each terminal bronchiole is called an "acinus". Miller (1950) defined the secondary lobule as an area surrounded by the interlobular septum (Figure 3). Reid's and Miller's lobules are not conceptually the same, because the interlobular septum is not constantly and uniformly observed within the lung, and the area surrounded by the septum ranges from 1 to 3 cm; in contrast, Reid's lobule is constantly and uniformly observed throughout the lung (Itoh et al 1993).

Terminal bronchioles branch off respiratory bronchioles which have walls with pores of alveoli. After 2 to 3 branches of respiratory bronchioles, the number of alveolar fenestrations increases gradually and these then change into alveolar ducts and sacs (Figure 4). The airway is essentially accompanied by the pulmonary artery, even at the level of secondary pulmonary lobules. The area around the terminal bronchiole and the 1st ordered respiratory bronchiole is called the "centrilobular portion" or "centriacinar portion" (Spencer 1985) (Figure 5). The pulmonary vein runs between the pulmonary segment and connects to the interlobular septum, which forms peripheral connective tissue together with the visceral pleura. The distance from the centrilobular portion to the peripheral structure, including the interlobular septum, pulmonary vein and pleura, is constant at about 2.5 mm (Itoh et al 1978; Murata et al 1986).

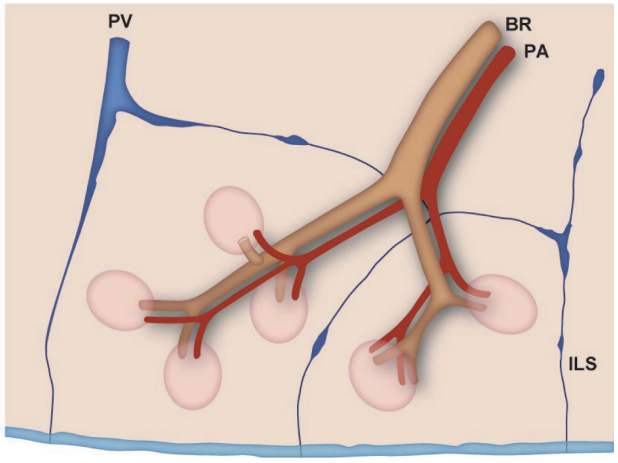

Figure 5 Centrilobular areas. Diagram showing the centrilobular areas, which correspond to the areas around the tips of terminal bronchioles and 1st respiratory bronchioles. Copyright © 1989. Modified with permission from Murata K, Khan A, Herman PG. 1989. Pulmonary parenchymal disease: evaluation with high-resolution CT. *Radiology*, 170:629–35.

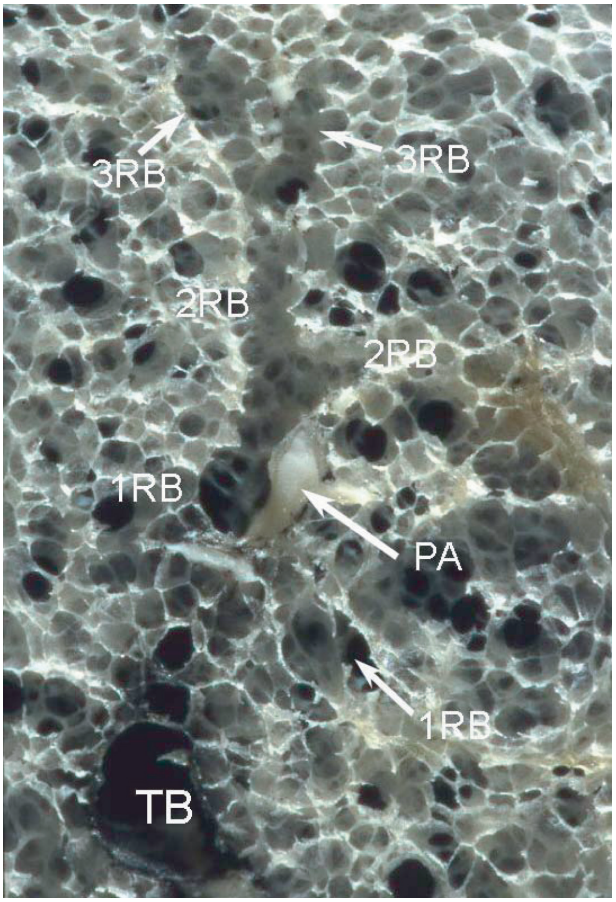

Figure 4 Terminal and respiratory bronchioles. Specimen photograph demonstrating ramification of the two 1st respiratory bronchioles (1RB) from the terminal bronchiole (TB). The respiratory bronchiole wall has alveolar pores. After branching of the respiratory bronchiole 2 to 3 times (2RB, 3RB), the number of alveolar fenestrations increases gradually and these eventually change into the alveolar duct and then the alveolar sac.

Visualization of peripheral lung structure by HRCT

In general, HRCT can be used to visualize an airway with a diameter larger than 2 mm, which corresponds to sub-subsegmental bronchi (Murata et al 1986). These bronchi are generally located in the inner two-thirds of the lung field (Murata et al 1986). In the distal lung field, the course of the airway can be recognized from the branching structure of the pulmonary artery that accompanies the airway. CT shows the pulmonary artery down to a caliber of 200 μm (Murata et al 1986). This portion corresponds to the level of the tip of the terminal bronchioles and the 1st respiratory bronchioles (Itoh et al 1978, Murata et al 1986). Therefore, a centrilobular region can be recognized as an area around the tip of the visible pulmonary artery (Figures 6, 7). Centrilobular abnormalities always have a distance of about 2.5 mm from the perilobular structure, including interlobular septum, pleura and large pulmonary vessels (Murata et al 1986, 1989). Recent HRCT with thinner collimation (0.5–1.0 mm) has more powerful

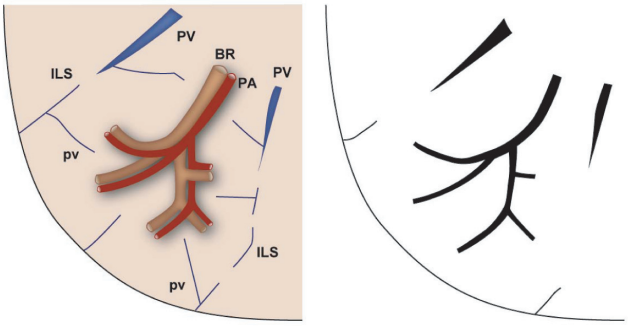

Figure 6 Structures of the peripheral lung that can be observed with HRCT. Right side: structure of the secondary lobule. Left side: structures visible on HRCT. Intralobular bronchioles cannot be seen. The smallest intralobular arteries that can be seen on HRCT are approximately 0.2 mm in diameter, which corresponds to the level of the tip of the terminal bronchiole and the 1st respiratory bronchiole. Therefore, the centrilobular portion can be seen as an area around the tip of the visible pulmonary artery on HRCT. Intralobular (interacinar) venules cannot be observed.
Abbreviations: BR, bronchus; HRCT, high resolution computed tomography; PA, pulmonary artery; PV, pulmonary vein; pv, intralobular (interacinar) venule; ILS, interlobular septum.

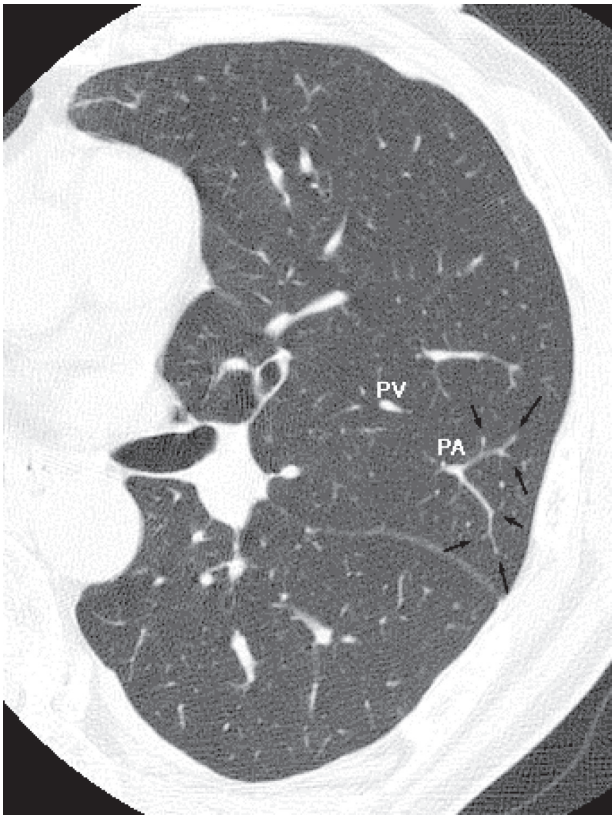

Figure 7 HRCT of the normal lung. The pulmonary artery supplies two secondary lobules, and arrows indicate branching of the intralobular pulmonary arteries. The corresponding airways cannot be seen.
Abbreviations: HRCT, high resolution computed tomography; PA, pulmonary artery, PV, pulmonary vein.

resolution for demonstration of peripheral lung structures, in which the distance between the most distal visible pulmonary artery and pleura is about 1–1.5 mm and that between the most distal visible airway and pleura is about 1.5 cm. The former corresponds to the level of 2nd respiratory bronchioles and the latter to prelobular bronchi (Takahashi et al 2002).

Classification of pulmonary emphysema

Pulmonary emphysema can be classified into three major subtypes based on the disease distribution within secondary pulmonary lobules (Stern and Frank 1994; Thurlbeck and Müller 1994): centriacinar emphysema, panacinar emphysema, and distal acinar emphysema (Figure 8). The relationships among these types of pulmonary emphysema and how each type is formed have yet to be clarified. The subtypes of emphysema can usually be determined in mild or moderate cases, but classification into anatomic subtypes becomes more difficult by CT and pathology as emphysema becomes more severe, with even highly trained and experienced pathologists sometimes disagreeing on the classification (Mitchell et al 1970). Centriacinar and panacinar emphysema can also coexist in the same patient; for example, with centriacinar emphysema in the upper lobe and panacinar emphysema in the lower lobe (Mitchell et al 1970).

Centriacinar emphysema

Centriacinar emphysema is the commonest type of pulmonary emphysema and is characterized by an enlargement of the centriacinar airspace, with the effect mainly occurring in proximal respiratory bronchioles, leaving normal distal alveolar ducts and sacs (Leopold and Gough 1957). The disease mainly involves the second and third respiratory bronchioles, and the severity of destruction of the lung parenchyma usually differs from lobule to lobule (Leopold and Gough 1957). Development of centriacinar emphysema is believed to be closely related to cigarette smoking and dust inhalation (ATS 1962; Finkelstein et al 1995; Cosio Piqueras et al 2001; Pauwels et al 2001; Satoh et al 2001), and most emphysema observed in heavy smokers is centriacinar emphysema (Thurlbeck 1963). The disease is usually distributed to the upper lobe or the superior segment of the lower lobe (Figure 9). The precise reasons for this distribution are unclear, but may include regional differences in perfusion, transit time of leukocytes, clearance of deposited dust, and pleural pressure (Gurney 1991). The inner zone is more severely affected than the outer zone, which may be explained by zonal differences in respiratory kinetics and lymph flow (Nakano et al 1999).

The characteristic appearance of a gross specimen of centriacinar emphysema is pigmentation (anthracosis) in a patchy

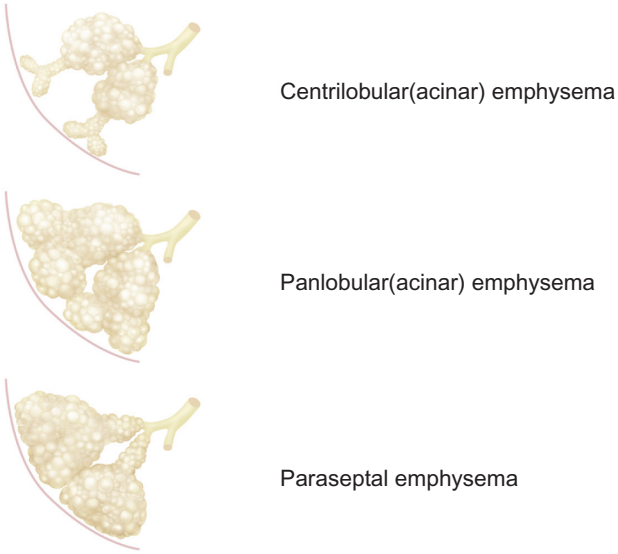

Figure 8 Subtypes of pulmonary emphysema.

fashion in the inner zone of the lung (Figure 10). This is one of the clues shows that centriacinar emphysema is closely associated with inhaled exogenous dust. The pigmented area corresponds to centriacinar dilatation of the airspace, but this area is not a simple unilocular space and is composed of aggregated and dilated small air spaces (Figures 11, 12). The surrounding lung parenchyma shows a normal appearance, but there is no border structure between these regions. Therefore, HRCT in early centriacinar emphysema shows evenly distributed centrilobular tiny areas of low attenuation with ill-defined borders (Naidich et al 1982) (Figure 13). Aggregation of the dilated small airspaces is observed as a single air space since this feature is beyond the spatial resolution of CT. With enlargement of the dilated airspace, the surrounding lung parenchyma is compressed, which enables a clear border to be observed between the emphysematous area and normal lung (Naidich et al 1982) (Figures 14, 15). Since the disease progresses from the centrilobular portion, the normal lung parenchyma in the perilobular portion tends to be preserved, even in advanced

Figure 9 Distribution of centriacinar emphysema. Photograph of an inflated and fixed lung showing emphysematous foci with anthracosis mainly distributed in the upper lobe and superior segment of the lower lobe (*).

Figure 10 Distribution of centriacinar emphysema. Photograph of an inflated and fixed lung showing emphysematous foci with anthracosis mainly observed in the inner zone of the lung.

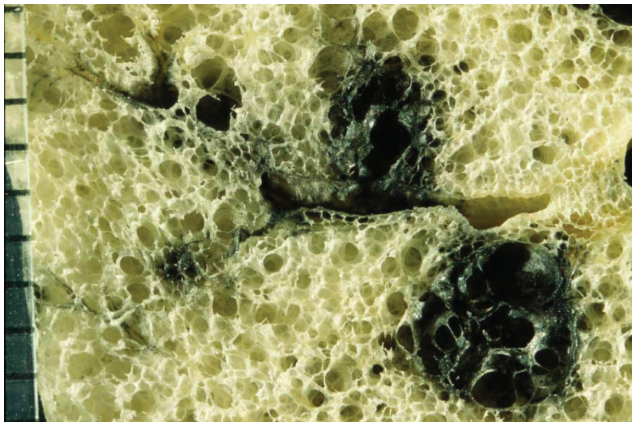

Figure 11 Centriacinar emphysema. Magnified photograph of emphysematous foci showing aggregation of an enlarged airspace with anthracosis. There is no bordering structure between the emphysematous space and surrounding lung parenchyma.

pulmonary emphysema (Figure 16). It is not uncommon for the lung parenchyma to be subtly preserved near the large airway and vessel in a case of severe emphysema, which indicates that the disease originated from the centrilobular portion (Figure 17). To understand the disease distribution, it is important to recognize the borders of the large airway and vessel as perilobular structures. The caliber of the vessel in the involved area decreases, which may be attributable to redistribution of pulmonary blood flow to the uninvolved area.

It is a controversial issue whether fibrosis is present in the histology of pulmonary emphysema, although the definition of the National Heart, Lung and Blood Institute notes the absence of obvious fibrosis (Cardoso et al 1993; Lang et al 1994). Most pulmonary pathologists notice that

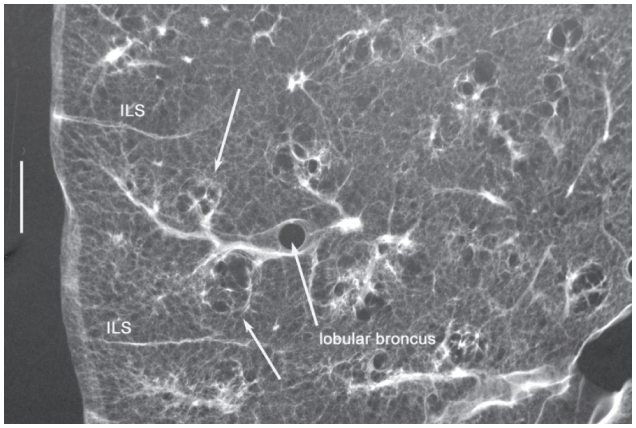

Figure 12 Centriacinar emphysema. Contact radiograph of an inflated fixed lung demonstrating low attenuation in the centriacinar area (arrow). Note that distances between the centriacinar portions and perilobular portions are constant at 2.5 mm. The bar indicates 5 mm.
Abbreviation: ILS: interlobular septum.

Figure 13 Early stage of centriacinar emphysema. High resolution computed tomography demonstrating numerous tiny low attenuation areas (LAAs) throughout the lung field. Note that each LAA does not have a clear wall.

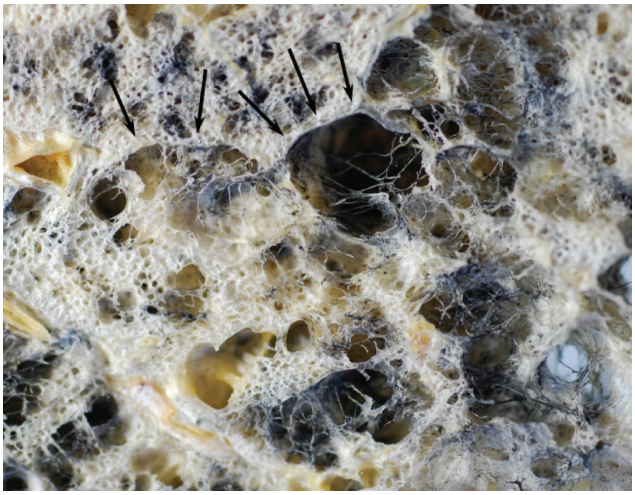

Figure 14 Moderately progressed centriacinar emphysema. Photograph of an inflated and fixed lung demonstrating that the surrounding lung parenchyma is compressed with enlargement of the dilated air spaces, producing a clear border of the emphysematous space (arrows).

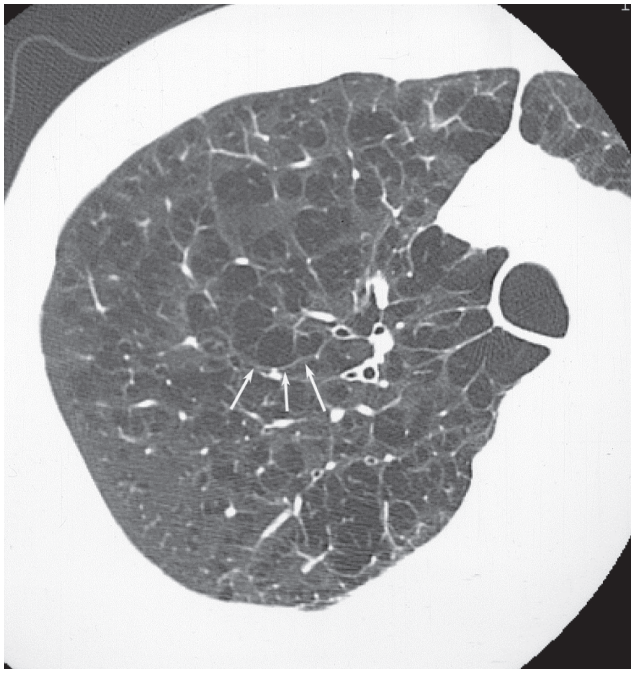

Figure 15 Moderately progressed centriacinar emphysema. On high resolution computed tomography, a "wall" structure is observed at the periphery of the emphysema (arrows), composed of compressed lung tissue and perilobular vessels.

Figure 17 Advanced centriacinar emphysema. It is very difficult to assess the subtype of emphysema using high resolution computed tomography. However, a small area of preserved normal lung can be observed around the large bronchovascular bundle and pulmonary vein, which indicates that this emphysema originated from the centriacinar area (arrow).

some degree of fibrosis is found around the emphysematous region (Cardoso et al 1993; Lang et al 1994), but how these fibrotic changes are reflected on HRCT images of pulmonary emphysema is unknown (Tonelli et al 1997).

Panacinar emphysema

Panacinar emphysema is characterized by a uniform dilatation of the air space from the respiratory bronchioles to the alveoli, resulting in evenly distributed emphysematous changes within secondary lobules (acini) (Thurlbeck 1995). In a gross specimen of a normal lung, the lumen of the alveolar ducts and respiratory bronchioles are slightly larger than surrounding normal alveoli (Heppleston and Leopold 1961; Thurlbeck 1963). In very early panacinar emphysema, this contrast tends to diminish with an increase in the size of the alveolar space and a "monotonous" appearance is apparent (Thurlbeck 1995). Alpha 1-antitrypsin deficiency is thought to be a major cause of panacinar emphysema, but the incidence is very low (Eriksson 1965). Other etiologies, including Swyer-James syndrome (Swyer and James 1953; Macleod 1954) and ritalin abuse, have been reported (Stern et al 1994), but most cases observed in surgical or autopsy specimens are unrelated to these conditions. Features that distinguish panacinar emphysema from centriacinar emphysema are as follows: the disease is dominant in the lower lung field, whereas the upper lung is mainly affected in centriacinar emphysema (Thurlbeck 1963); the degree of lung inflation is greater than that in centriacinar emphysema; there is a tendency for the airway to be narrowed; and bullous formation is less frequently observed compared to centriacinar emphysema (Mitchell et al 1970).

Two types of disease distribution have been recognized in panacinar emphysema: a localized form and a diffuse form (Thurlbeck 1995) (Figure 18). The former has a multilobular distribution and the latter has a distribution that is not related to the zonal anatomy of the lung. The striking difference from

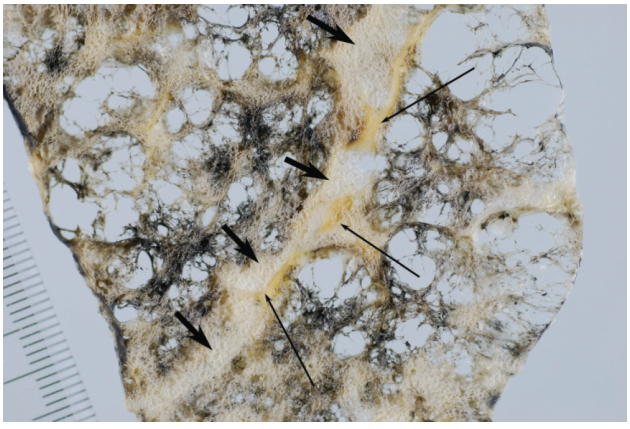

Figure 16 Advanced centriacinar emphysema. Photograph of an inflated and fixed lung showing that residual normal lung is clearly observed around the large vessels (arrows), even in progressed emphysema. The long arrows represent pulmonary veins.

Figure 18 Panacinar emphysema. An inflated-fixed lung does not demonstrate obvious anthracosis. Enlargements of airspaces are diffusely observed and in some areas the disease is bordered by the interlobular septum (arrow).

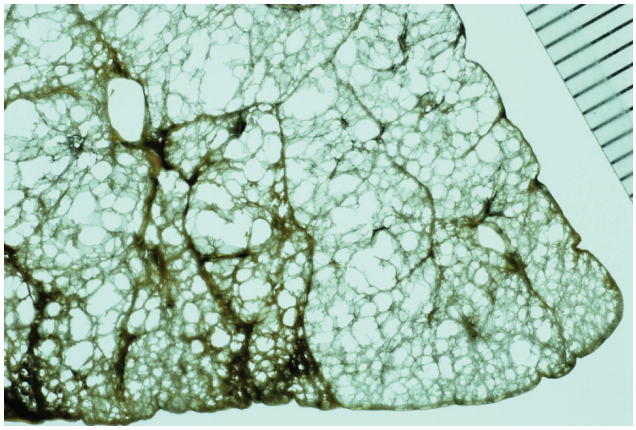

Figure 19 Panacinar emphysema. On the photograph of an inflated-fixed lung, airspaces are evenly enlarged throughout the secondary lobule, but the degree of enlargement is not necessarily the same within the lobule.

centriacinar emphysema is the low contrast to the neighboring normal lung (Stern and Frank 1994). The low attenuation of centriacinar emphysema is easily recognized on HRCT because of the contrast between the emphysematous region and the normal lung, whereas panacinar emphysema does not show a difference in intralobular attenuation because the entire lobule is involved to almost the same extent. Yamagishi and colleagues (1991) reported several CT-pathological observations in cases of panacinar emphysema, as follows: the low attenuation region is not evenly distributed within the lobule or lobule-by-lobule on HRCT, which is attributed to an uneven distribution of the degree of the disease; the caliber of the vessels in the involved area is decreased due to overinflation of the air space; the localized form of panacinar emphysema has a polygonal border, which represents the interlobular septum, and perilobular large vessels are observed at the border of the lesion (Figure 19); and the margin of the diffuse form of panacinar emphysema is ill defined, due to the inhomogeneity of the intralobular disease distribution in lobules located at the periphery of the lesion (Figures 20, 21).

Distal acinar or paraseptal emphysema

Distal acinar or paraseptal emphysema is characterized as an enlarged airspace at the periphery of acini (Thurlbeck 1995). The lesion is usually limited in extent, occurs most commonly along the dorsal surface of the upper lung (Figures 22, 23), and is often associated with fibrosis and may coexist with other types of emphysema. The patient is usually asymptomatic, but the condition is considered to be a cause of pneumothorax in young adults (Peters et al 1978; Lesur et al 1990).

Aging lung

The lung undergoes a set of morphological and functional changes with aging. These changes, which may also be the result of environmental pollutants rather than aging alone (Thurlbeck 1995), include dilatation of alveolar ducts and respiratory bronchioles without obvious destruction of the alveolar wall (Ryan et al 1965). This is not referred to as emphysema, since emphysema is defined as an abnormal

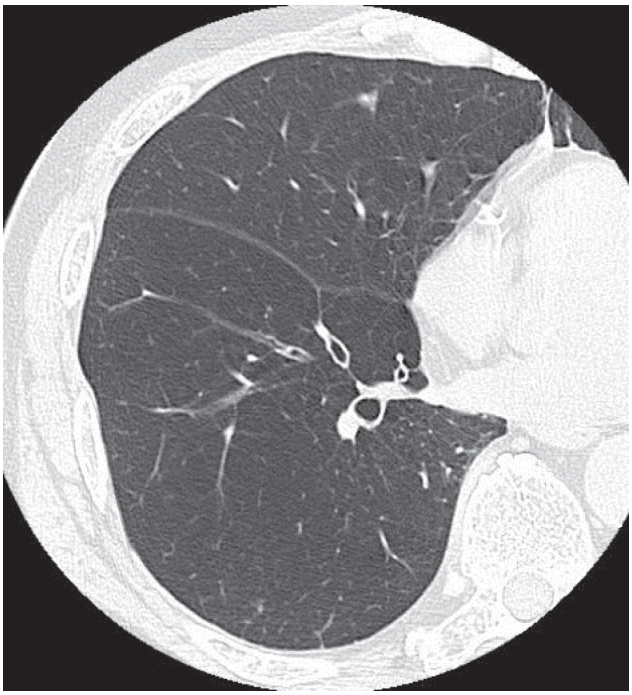

Figure 20 Panacinar emphysema. On high resolution computed tomography, diffuse low attenuation changes are observed throughout the lung field. A localized LAA is not apparent.

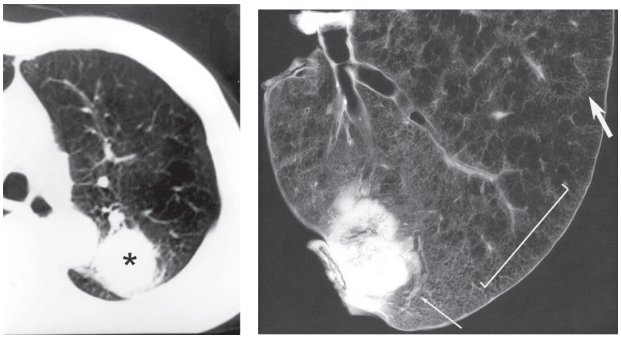

Figure 21 Panacinar emphysema in a case with bronchogenic carcinoma.
a. Preoperative CT showing a diffuse low attenuation area in the left upper lobe. The lung tumor is also observed in the dorsal portion of the left upper lobe (asterisks).
b. Contact photograph of the resected specimen. Panacinar emphysema is diffusely observed, but the dorsal area has a normal appearance. There is no clear border between these regions and the change is gradual (bar). The caliber of the pulmonary artery in the involved area is markedly narrowed (large arrow) compared to that in normal lung (small arrow).

enlargement of the air space accompanied by destruction of the alveolar walls. In contrast to dilatation of alveolar ducts and respiratory bronchioles, the size of the alveoli is reduced, a process that has been referred to as "ductectasia" (Ryan et al 1965) (Figures 24, 25). This aging change is reflected in the "rounds out" configuration of the lung in which the anteroposterior diameter is increased (Anderson et al 1964). HRCT findings of the aging lung have not been established, probably because the difference in attenuation accompanying the changes is small.

Imaging topics related to pulmonary emphysema

Phenotyping of COPD and imaging

COPD is considered to be a chronic inflammatory process throughout the airway and lung parenchyme, allowing

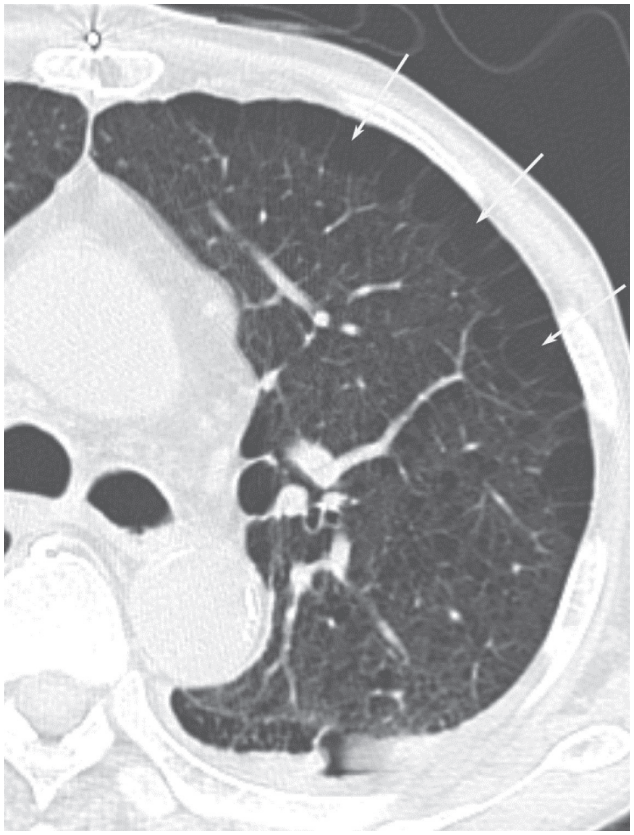

Figure 23 Distal acinar emphysema. High resolution computed tomography showing subpleural airspaces (arrows) and associated centrilobular emphysema.

definition of two phenotypes involving primarily parenchymal disease (emphysema) and primarily airway disease (Nakano et al 2002; Hoffman et al 2006). These two pathologies frequently coexist in a diseased lung. Pathological changes of the large airway include enlarged mucus-secreting glands

Figure 22 Distal acinar emphysema. Photograph of an inflated and fixed lung specimen showing subpleural airspaces with smooth wall structures.

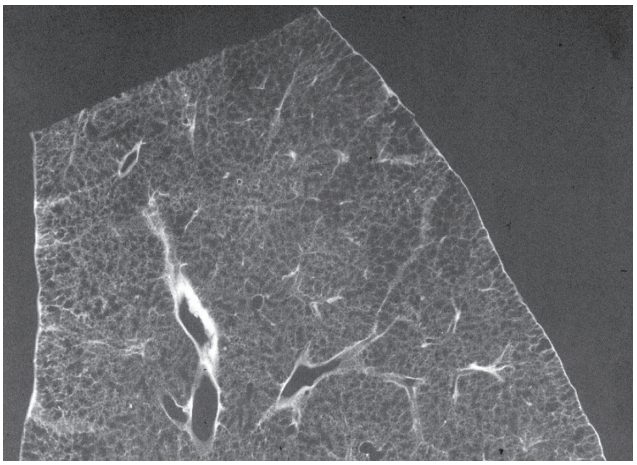

Figure 24 Aging lung. Contact radiograph of an inflated and fixed lung specimen showing a homogenous distribution of enlarged airspaces.

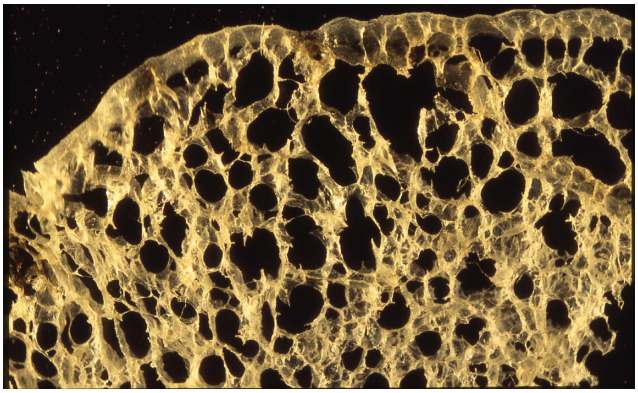

Figure 25 Aging lung. Magnified photograph of a specimen showing slight enlargement of respiratory bronchioles and alveolar ducts. Clear destruction of the alveolar wall is not apparent.

and an increase in the number of goblet cells with mucus hypersecretion (Pauwels et al 2001). In the peripheral airways, chronic inflammation leads to repeated cycles of injury and repair of the airway wall (Pauwels et al 2001), and the repair process results in structural remodeling of the airway wall (Pauwels et al 2001). Quantitative measurement of the airway by HRCT is a promising method for evaluation of the inflammatory condition of the airway in COPD, and recent studies have shown that HRCT can be used to divide COPD patients into groups with predominant lower lung attenuation or thickening and narrowing of the airway, although many subjects have both abnormalities (Nakano et al 2002 Hoffman et al 2006) (Figure 26).

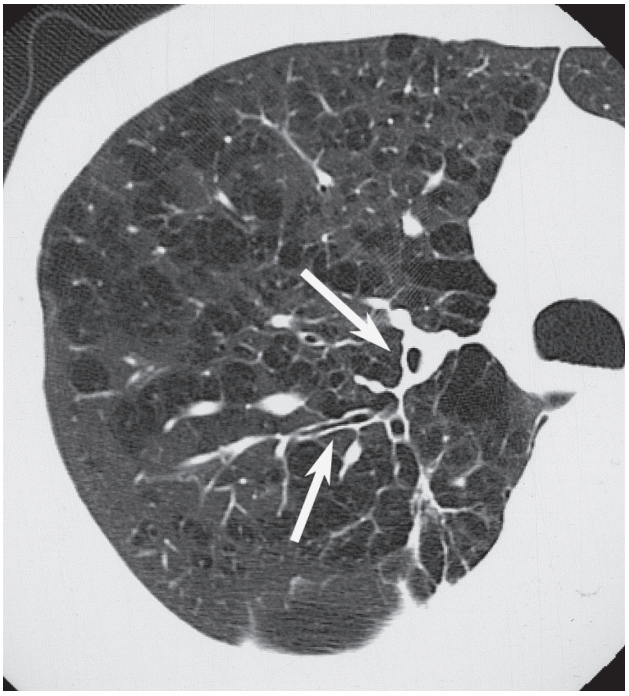

Figure 26 Thickening of the bronchial wall in cases of pulmonary emphysema. High resolution computed tomography showing thickening of the bronchial wall and narrowing of the lumen (arrows).

Combined pulmonary fibrosis and pulmonary emphysema

Although not completely established, some patients with pulmonary emphysema in the upper lung field are reported to have simultaneous pulmonary

fibrosis in the lower lung field (Wiggins et al 1990; Cottin et al 2005; Lundblad et al 2005; Grubstein et al 2005; Mura et al 2006) (Figure 27). Cottin and colleagues (2005) performed a retrospective analysis of 61 patients with emphysema of the upper zones and diffuse parenchymal lung disease with fibrosis of the lower zones of the lung on chest CT. These patients were characterized by subnormal spirometry, severe impairment of gas exchange, a high prevalence of pulmonary hypertension, and poor survival. The patients were almost exclusively male and all were current or ex-smokers. The pathophysiology of combined pulmonary fibrosis and pulmonary emphysema (CPFE) is unknown, but it is speculated that both emphysema and fibrosis may be related to a common environmental trigger or a genetic susceptibility factor. Smoking plays a central role and overexpression of TNF-α due to smoking may be important in producing emphysema and pulmonary fibrosis (Cottin et al 2005; Lundblad et al 2005; Gauldie et al 2006).

Bronchogenic carcinoma associated with bullous lung disease

Bullous lung is a risk factor for bronchogenic carcinoma, with a 32 times higher risk of developing bronchogenic carcinoma in patients with BLD compared with those without BLD (Stoloff et al 1971). Radiological diagnosis

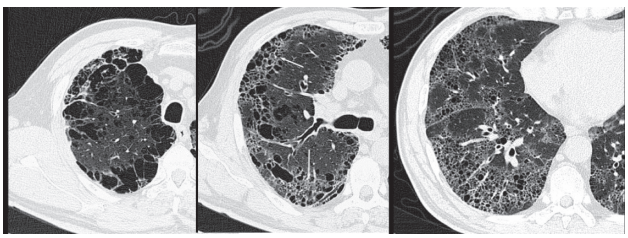

Figure 27 Combined pulmonary fibrosis and pulmonary emphysema (CPFE) in a 59-year-old male who was a heavy smoker: High resolution computed tomography images.
In the upper lung field (**a**), a prominent bullous change is apparent. In the middle lung field (**b**), tiny air cysts (arrows) with ground-glass opacity are present in addition to the bullous changes. In the lower lung field (**c**), distributed tiny air cysts with definable walls and ground-glass opacity are apparent. These features are consistent with interstitial fibrosis rather than pulmonary emphysema.

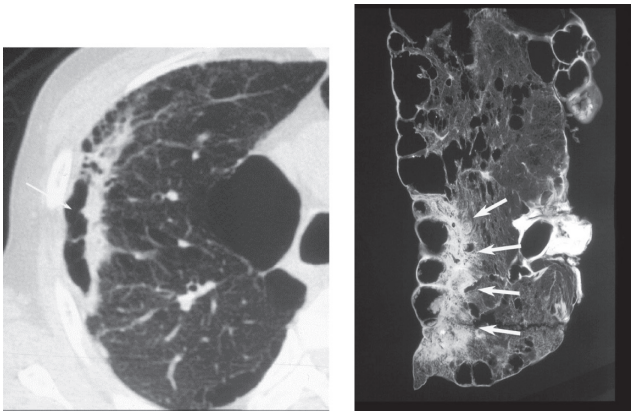

Figure 28 Occurrence of bronchogenic carcinoma with emphysema in a 68-year-old male. High resolution computed tomography A subpleural band-like structure is observed with adjacent emphysematous changes (arrow). Postinflammatory fibrotic tissue was suspected, but malignancy could not be confidently excluded and thoracotomy was performed. Contact radiograph of a specimen showing that the tumor grew along the surface of the emphysematous space (arrows). The pathological diagnosis was well-differentiated adenocarcinoma. Copyright © 2006, Lippincott Williams & Wilkins. Reproduced with permission from Maki D, Takahashi M, Murata K, et al. 2006. Computed tomography appearances of bronchogenic carcinoma associated with bullous lung disease. *J Comput Assist Tomogr*, 30:447–52.

of bronchogenic carcinoma is based on the shape, density, and interface with surrounding lung parenchyma. However, these morphologies in bronchogenic carcinoma can be changed by underlying emphysematous changes, including influences on the extent of the tumor and the tumor – lung interface. In the normal lung field, bronchogenic carcinoma tends to grow globally, but this is not always true if the tumor occurs with pulmonary emphysema. Since tumors tend to grow along the intervening normal lung, bizarre shapes are often observed. Some cases have findings that are similar to those of post-inflammatory fibrotic changes because the tumor extends along the emphysematous lesion, resulting in a thickened band-like structure (Figure 28). Nodular form of the bronchiolar alveolar carcinoma has an ill-defined border because tumor cells in the periphery grow along the alveolar wall with preserving alveolar air space. However, the interface can be well defined if the dilated air space is neighboring to it. On CT, attention should be paid in the interpretation for mass or nodule in the wall of the bulla because they frequently lack the characteristic appearance of bronchogenic carcinoma.

Conclusion

HRCT plays an important role for analyzing pathologies of pulmonary emphysema not only in its morphological aspect but also in the assessment of severity. HRCT will also contribute the phenotyping of COPD, such as primarily parenchymal disease and primarily airway disease.

References

Anderson WF, Anderson AE Jr, Hernandez JA, et al. 1964. Topography of aging and emphysematous lungs. *Am Rev Respir Dis*, 90:411–23.

[ATS] Committee on Diagnostic Standards for Nontuberculous Respiratory Diseases, American Thoracic Society. 1962. Definitions and classification of chronic bronchitis, asthma, and pulmonary emphysema. *Am Rev Respir Dis*, 85:762–9.

Cardoso WV, Sekhon HS, Hyde DM, et al. 1993. Collagen and elastin in human pulmonary emphysema. *Am Rev Respir Dis*, 147:975–81.

Cosio Piqueras MG, Cosio MG. 2001. Disease of the airways in chronic obstructive pulmonary disease. *Eur Respir J Suppl*, 34:41s–49s.

Cottin V, Nunes H, Brillet PY, et al. 2005. Combined pulmonary fibrosis and emphysema: a distinct underrecognised entity. *Eur Respir J*, 26:586–93.

Eriksson S. 1965. Studies in alpha-1-antitrypsin deficiency. *Acta Medica Scandinavica*, 177(Suppl 432):1–85.

Finkelstein R, Ma HD, Ghezzo H, et al. 1995. Morphometry of small airways in smokers and its relationship to emphysema type and hyperresponsiveness. *Am J Respir Crit Care Med*, 152:267–76.

Gauldie J, Kolb M, Ask K, et al. 2006. Smad3 signaling involved in pulmonary fibrosis and emphysema. *Proc Am Thorac Soc*, 3:696–702.

Grubstein A, Bendayan D, Schactman I, et al. 2005. Concomitant upper-lobe bullous emphysema, lower-lobe interstitial fibrosis and pulmonary hypertension in heavy smokers: report of eight cases and review of the literature. *Respir Med*, 99:948–54.

Grumelli S, Corry DB, Song LZ, et al. 2004. An immune basis for lung parenchymal destruction in chronic obstructive pulmonary disease and emphysema. *PLoS Med*, 1:e8.

Gurney JW. 1991. Cross-sectional physiology of the lung. *Radiology*, 178:1–10.

Heppleston AG, Leopold JG. 1961. Chronic pulmonary emphysema: anatomy and pathogenesis. *Am J Med*, 31:279–91.

Hoffman EA, Simon BA, McLennan G. 2006. State of the Art. A structural and functional assessment of the lung via multidetector-row computed tomography: phenotyping chronic obstructive pulmonary disease. *Proc Am Thorac Soc*, 3:519–32.

Itoh H, Murata K, Konishi J, et al. 1993. Diffuse lung disease: pathologic basis for the high-resolution computed tomography findings. *J Thorac Imaging*, 8:176–88.

Itoh H, Tokunaga S, Asamoto H, et al. 1978. Radiologic-pathologic correlations of small lung nodules with special reference to peribronchiolar nodules. *AJR Am J Roentgenol*, 130:223–31.

Lang MR, Fiaux GW, Gillooly M, et al. 1994. Collagen content of alveolar wall tissue in emphysematous and non-emphysematous lungs. *Thorax*, 49:319–26.

Leopold JG, Gough J. 1957. The centrilobular form of hypertrophic emphysema and its relation to chronic bronchitis. *Thorax*, 12:219–35.

Lesur O, Delorme N, Fromaget JM, et al. 1990. Computed tomography in the etiologic assessment of idiopathic spontaneous pneumothorax. *Chest*, 98:341–7.

Lundblad LK, Thompson-Figueroa J, Leclair T, et al. 2005. Tumor necrosis factor-alpha overexpression in lung disease: a single cause behind a complex phenotype. *Am J Respir Crit Care Med*, 171:1363–70.

Macleod WM. 1954. Abnormal transradiancy of one lung. *Thorax*, 9:147–53.

Miller WS. 1950. The acinus. In: Miller WS (ed). The Lung. 2nd ed. Charles C. Thomas Springfield, pp. 203–5.

Mitchell RS, Silvers GW, Goodman N, et al. 1970. Are centrilobular emphysema and panlobular emphysema two different diseases? *Hum Pathol*, 1:433–41.

Mura M, Zompatori M, Pacilli AM, et al. 2006. The presence of emphysema further impairs physiologic function in patients with idiopathic pulmonary fibrosis. *Respir Care*, 51:257–65.

Murata K, Itoh H, Todo G, et al. 1986. Centrilobular lesions of the lung: demonstration by high-resolution CT and pathologic correlation. *Radiology*, 161:641–5.

Murata K, Khan A, Herman PG. 1989. Pulmonary parenchymal disease: evaluation with high-resolution CT. *Radiology*, 170:629–35.

Naidich DP, McCauley DI, Khouri NF, et al. 1982. Computed tomography of bronchiectasis. *J Comput Assist Tomogr*, 6:437–44.

Nakano Y, Müller NL, King GG, et al. 2002. Quantitative assessment of airway remodeling using high-resolution CT. *Chest*, 122(6 Suppl):271S–275S.

Nakano Y, Sakai H, Muro S, et al. 1999. Comparison of low attenuation areas on computed tomographic scans between innerand outer segments of the lung in patients with chronic obstructive pulmonary disease: incidence and contribution to lung function. *Thorax*, 54:384–9.

Pauwels RA, Buist AS, Calverley PM, et al. 2001. Global strategy for the diagnosis, management, and prevention of chronicobstructive pulmonary disease. NHLBI/WHO Global Initiative for ChronicObstructive Lung Disease (GOLD) Workshop summary. *Am J Respir Crit Care Med*, 163:1256–76.

Peters RM, Peters BA, Benirschke SK, et al. 1978. Chest dimensions in young adults with spontaneous pneumothorax. *Ann Thorac Surg*, 25:193–6.

Reid L.1958. The secondary lobule in the adult human lung with special reference to its appearance in bronchograms. *Thorax*, 13:110–15.

Ryan SF, Vincent TN, Mitchell RS, et al. 1965. Ductectasia; an asymptomatic pulmonary change related to age. *Med Thorac*, 22:181–7.

Satoh K, Kobayashi T, Misao T, et al. 2001. CT assessment of subtypes of pulmonary emphysema in smokers. *Chest*, 120:725–9.

Snider GL, Kleinerman J, Thurlbeck WM, et al. 1985. The definition of emphysema. Report of a National Heart, Lung, and Blood Institute, Division of Lung Diseases workshop. *Am Rev Respir Dis*, 132:182–5.

Spencer H. 1985. Pathology of the lung. 4th ed. Oxford, England: Pergamon, pp. 571–81.

Stern EJ, Frank MS, Schmutz JF, et al. 1994. Panlobular pulmonary emphysema caused by i.v. injection of methylphenidate (Ritalin): findings on chest radiographs and CT scans. *AJR Am J Roentgenol*, 162:555–60.

Stern EJ, Frank MS. 1994. CT of the lung in patients with pulmonary emphysema: diagnosis, quantification, and correlation with pathologic and physiologic findings. *AJR Am J Roentgenol*, 162:791–8.

Stoloff IL, Kanofsky P, Magilner L. 1971. The risk of lung cancer in males with bullous disease of the lung. *Arch Environ Health*, 22:163–7.

Swyer PR, James GC. 1953. A case of unilateral pulmonary emphysema. *Thorax*, 8:133–6.

Takahashi M, Nitta N, Takazakura R, et al. 2002. 0.5 mm thickness HRCT: How precisely are the normal and abnormal lung structures demonstrated? Part 1: Fundamental study using inflated and fixed lung specimen. *Radiology*, 225:144–5.

Thurlbeck WM, Müller NL. 1994. Emphysema: definition, imaging, and quantification. *AJR Am J Roentgenol*, 163:1017–25.

Thurlbeck WM. 1963. The incidence of pulmonary emphysema, with observations on the relative incidence and spatial distribution of various types of emphysema. *Am Rev Respir Dis*, 87:206–15.

Thurlbeck WM. 1995. Chronic airflow obstruction. In: Thurlbeck WM, Churg AM (ed). Pathology of the lung. 2nd Ed. New York: Thieme Medical Publishers, pp. 739–826.

Tonelli M, Stern EJ, Glenny RW. 1997. HRCT evident fibrosis in isolated pulmonary emphysema. *J Comput Assist Tomogr*, 21:322–3.

Tuder RM, Yoshida T, Arap W, et al. 2006. State of the art. Cellular and molecular mechanisms of alveolar destruction in emphysema: an evolutionary perspective. *Proc Am Thorac Soc*, 3:503–10.

Wiggins J, Strickland B, Turner-Warwick M. 1990. Combined cryptogenic fibrosing alveolitis and emphysema: the value of high resolution computed tomography in assessment. *Respir Med*, 84:365–9.

Wright JL, Churg A. 2007. Current concepts in mechanism of emphysema. *Toxicologic Pathology*, 35:111–15.

Yamagishi M, Koba H, Honma A, et al. 1991. [CT findings in panacinar emphysema.] *Nihon Kyobu Shikkan Gakkai Zasshi*, 29:1407–13. [Article in Japanese]